HHS Public Access

Author manuscript

J Control Release. Author manuscript; available in PMC 2021 September 10.

Published in final edited form as:

J Control Release. 2020 September 10; 325: 198–205. doi:10.1016/j.jconrel.2020.06.030.

Theranostic dendrimer-based lipid nanoparticles containing PEGylated BODIPY dyes for tumor imaging and systemic mRNA delivery in vivo

Hu Xiong[a,b], **Shuai Liu**[b], **Tuo Wei**[b], **Qiang Cheng**[b], **Daniel J. Siegwart**[b]

[a]Nankai University, Research Center for Analytical Sciences, Tianjin Key Laboratory of Biosensing and Molecular Recognition, College of Chemistry, Tianjin 300071, China

[b]The University of Texas Southwestern Medical Center, Department of Biochemistry, Simmons Comprehensive Cancer Center, Dallas, TX 75390, United States

Abstract

mRNA-based therapeutics have emerged as a promising approach to treat cancer. However, creation of theranostic strategies to both deliver mRNA and simultaneously detect cancer is an important unmet goal. Here, we report the development of theranostic dendrimer-based lipid nanoparticle (DLNP) system containing PEGylated BODIPY dyes (PBD) for mRNA delivery and near-infrared (NIR) imaging *in vitro* and *in vivo*. DLNPs formulated with a pH-responsive PBD-lipid produced 5- to 35-fold more functional protein than control DLNPs formulated with traditional PEG-lipid *in vitro* and enabled higher mRNA delivery potency *in vivo* at a low dose of 0.1 mg kg^{-1} when formulated with a PBD-lipid containing a BODIPY core, indole linker, and PEG length between 1000 and 5000 g/mol. Moreover, we found the intensity of mRNA expression in the liver correlated with the pKa of DLNPs, indicating that DLNPs with a pKa close to 6.3 could generally produce more protein in livers. Notably, 4A3-SC8&PEG2k**5d** formulated DLNPs successfully mediated mRNA expression in tumors and simultaneously illuminated tumors via pH-responsive NIR imaging. The described theranostic lipid nanoparticles that combine mRNA delivery and NIR imaging hold promise as an applicable future approach to simultaneously detect and treat cancer.

Graphical Abstract

Supplementary Material

Supplementary material includes Materials and Methods along with Supplemental Figures S1-17

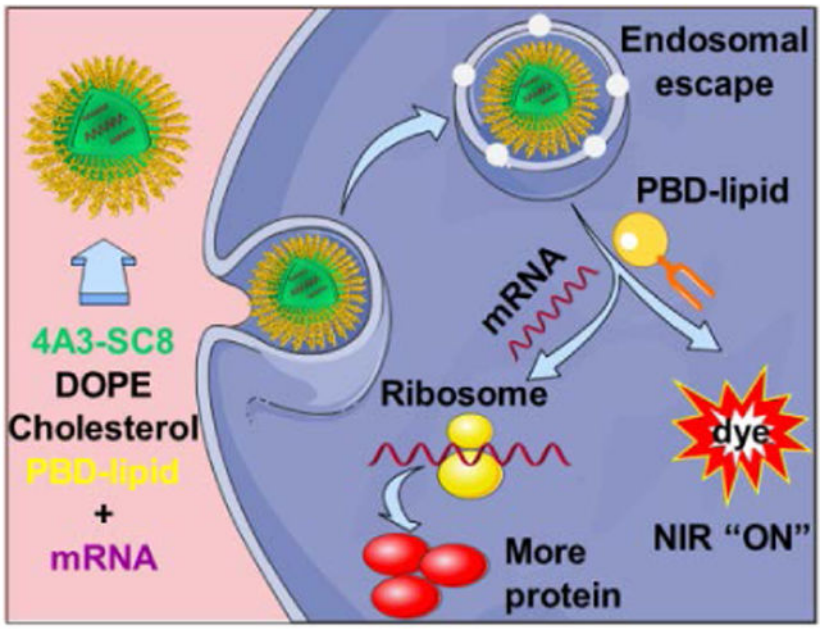

Theranostic nanomedicines have the potential to both detect cancer and provide therapeutically active drugs. Herein, a theranostic DLNP system containing PBD-lipids is developed for effective mRNA delivery and non-invasive NIR imaging. This unique combination of PDB-lipids with DLNPs enhanced mRNA production in cancer cells, mediated mRNA expression in tumors, and simultaneously illuminated tumors via pH-responsive NIR imaging.

Keywords

mRNA delivery; lipid nanoparticles; dendrimers; NIR imaging; theranostics

1. Introduction

Messenger RNA (mRNA)-based therapeutics have recently drawn great attention to treat many diseases caused by aberrant protein expression, ranging from genetic disorders to aggressive cancer [1-3]. Applications of mRNA include protein replacement therapy, cancer immunotherapy, vaccination, and gene editing [4-10]. Unlike DNA-based gene therapy that requires nuclear entry, mRNAs need only to reach the cytoplasm to produce functional proteins. mRNA-based protein replacement therapies would also not integrate into the host genome, which reduces risks of insertional mutagenesis [11]. Notably, mRNAs can be translated to many copies of protein, which is easier, cheaper, and carries a lower biosafety risk than direct protein therapy [3]. However, mRNA is a large, polyanionic, and single-stranded molecule that does not readily enter the cytoplasm and is generally unstable in blood circulation due to degradation by highly active RNases [12]. Thus, like DNA and siRNA delivery, the broad application of mRNA-based therapeutics is impeded by the lack of effective and safe delivery systems. Recently, ionizable lipid nanoparticles (LNPs) and polymers have been adapted for mRNA delivery *in vivo*, which can shield mRNA from RNases, prevent unwanted clearance, and promote cellular uptake [8-10, 13-22]. Although

significant advances have been made towards delivery, applications of mRNA drugs to cancer would greatly benefit from the ability to simultaneously detect and image tumors. Thus, the development of theranostic mRNA LNPs that can efficiently produce functional protein concurrent to tumor imaging is an exciting unmet challenge.

mRNA-loaded LNPs are composed of an ionizable cationic lipid, phospholipid (e.g. DOPE), cholesterol, and polyethylene glycol (PEG) lipid [3]. Each component plays an important role in efficient delivery of mRNA and stability of LNPs. The ionizable lipid is a key component that electrostatically binds negatively charged mRNA at low pH during mixing and subsequently facilitates cellular uptake and endosomal escape via charge acquisition [3, 23]. Therefore, extensive efforts have been devoted to developing lipid-like materials (e.g., DLin-MC3-DMA, C12-200, TT3, OF-02, ZA3-Ep10) for mRNA delivery through the use of combinatorial library screening [8, 13-17, 24, 25]. We previously reported a large library of >1500 dendrimer-based lipid nanoparticles (DLNPs) that could effectively deliver siRNAs/miRNAs to compromised livers and extend the survival of mice with aggressive liver cancer using a leading dendrimer 5A2-SC8 [26]. 5A2-SC8 DLNPs were further optimized to increase delivery potency of FAH mRNA *in vivo* by changing the molecular composition of LNP components [23]. DLNPs can also be tuned for tissue-specific mRNA delivery and CRISPR/Cas gene editing [27]. Since the ionizable cationic (dendrimer) lipid has the most influence on efficacy because it binds and releases RNAs, it is logical to conduct experiments aimed at discovering additional leading dendrimers that can be easily synthesized and purified for efficient mRNA delivery *in vitro* and *in vivo*.

As an additional key component of LNPs, PEG-lipids typically bear one hydrophilic PEG chain and two flexible hydrophobic alkyl tails to reduce LNP aggregation and nonspecific uptake by immune cells [28]. We previously developed pH-activatable PEGylated near-infrared (NIR) BODIPY probes that activate in breast cancer metastases by responding to low pH and provide high tumor-to-liver contrast [29, 30] when administered on their own as water-soluble probes. Comparing to typical PEG-lipids, we realized that PEGylated BODIPY dyes (PBD) bear two hydrophilic PEG chains and one rigid hydrophobic BODIPY tail, which offers structural similarity to traditional PEG-lipids used in LNPs.

We therefore hypothesized that tumor activatable PBDs could be utilized as surface stabilizing PEG-lipids in DLNPs to create theranostic nanoparticles for image-guided gene delivery. Moreover, activatable PBDs may not only improve DLNP formulations due to the rigid planar BODIPY tail but also promote intracellular mRNA release as the pH decreases during endosomal maturation because PBDs are pH-responsive. PBD-lipids also offer tunability due to their modular design consisting of a BODIPY core, aryl linker, and PEG length. Since the chemical identity and the molar ratio of each molecule within self-assembled LNPs affects stability and efficacy [8, 16, 17, 23, 25, 27, 31-39], including variation of hydrophobic components (e.g. cholesterol) [34, 35] and phospholipids, PEG-lipid chemical structure may also significantly impact functional delivery of mRNA. Although fluorescently tagged mRNAs have been incorporated into LNPs to track biodistribution [14, 19], theranostic mRNA delivery using pH-activatable “turn on” PBDs that are not incorporated to track an LNP but instead become an intrinsic part of the LNPs for both mRNA delivery and tumor imaging have not been realized.

Inspired by these observations, we herein developed a theranostic LNP platform combining degradable DLNPs and PBD-lipids for efficient mRNA delivery and non-invasive NIR imaging *in vitro* and *in vivo* (Figure 1). Since the ionizable cationic (dendrimer) lipid has the most influence on efficacy because it binds and releases RNAs, we examined a series of dendrimers for potential incorporation in PBD DLNPs. Other DLNPs that can effectively deliver siRNAs have not been investigated for mRNA delivery *in vitro* or *in vivo*, which may have modulated activity when combined into theranostic LNPs. In this work, we identified two leading dendrimers termed 4A3-SC8 and 5A4-SC8 that have not been used for mRNA delivery before. 4A3-SC8 and 5A4-SC8 that were easily synthesized and purified, which could form DLNPs to efficiently deliver mRNA to the liver after systemic administration. The effects of BODIPY core, aryl linker, and PEG length in PBD-lipids on DLNP potency of mRNA delivery were systemically investigated. It was determined that these factors dramatically affected mRNA delivery and expression. DLNPs formulated with a pH-responsive PBD-lipid could effectively deliver mRNA to cells and produce more protein in the cytoplasm, approximately over 5- to 35-fold increase compared to traditional DLNP formulations using 1,2-dimyristoyl-rac-glycero-3-methoxypolyethylene glycol-2000 (PEG-DMG) [23]. In addition, DLNPs formulated with a PBD-lipid bearing “always-on” BODIPY core, indole linker, and PEG length between 1000 and 5000 g/mol enabled higher mRNA delivery potency *in vivo*. Importantly, the intensity of mRNA expression correlated with the pKa of DLNPs. Notably, 4A3-SC8&PEG2k**5d** DLNP could successfully mediate luciferase mRNA expression in the livers and tumors and simultaneously illuminate the tumors by pH-activatable NIR imaging. This initial concept of a theranostic LNP system for combined mRNA delivery and NIR imaging may be useful to deliver a variety of mRNAs, including those encoding for tumor suppressor genes, to tumors for theranostic imaging and treatment.

2. Materials and methods

Full materials and methods appear in the Supplementary Information.

3. Results and discussion

3.1. Design and optimization of theranostic NIR PBD DLNPs

Water soluble pH-activatable NIR PBDs have been established with the capability to effectively image primary tumors and successfully detect metastatic breast cancer including liver and bone micrometastases with high tumor-to-normal (T/N) contrast when administered IV on their own [29, 30]. However, pH-activatable NIR PBDs are water-soluble dyes and cannot deliver mRNA themselves. Here, we hypothesized that they could be investigated for nucleic acid delivery as “PEG-lipids” to stabilized LNPs. PEG-lipids are essential intrinsic components of LNPs that benefit mRNA delivery *in vivo* by anchoring hydrophilic PEG on the surface of formulated mRNA LNPs, which protects LNPs from aggregation and nonspecific uptake. On the contrary, too much PEG on the surface may decrease cellular uptake [20, 23]. Thus, we herein explored the chemistry of PBD lipids and LNP formulation parameters for creation of theranostic nanoparticles.

DLNPs are dendrimer-based lipid nanoparticles containing PEG-DMG that can deliver RNAs [23, 26, 27, 37, 40, 41] . In this paper, we combined NIR PBDs and DLNPs to create

theranostic nanoparticles that can both deliver mRNA and “turn on” in tumors. Because different dendrimers have not been tested for mRNA delivery, we examined a series of dendrimers combined with NIR PBDs (Figure 1a). Because NIR PBDs have different chemical structures than traditionally used PEG-DMG, we optimized the molar ratio of NIR PBDs for this new system. In addition, since PEG2k**5c** is pH-activatable and able to successfully image tumors with high T/N contrast ratio [29, 30], we explored it as a representative PBD-lipid for optimization of mRNA delivery.

To determine optimal formulation conditions for mRNA delivery using PBD-lipids, we evaluated luciferase (Luc) mRNA delivery efficacy of 5A2-SC8 DLNPs formulated with 1.64%, 3.23%, 4.76%, 7.69%, and 11.76% PEG2k**5c**, respectively. The highest efficacy was reached at 3.23% PEG2k**5c** (5A2-SC8/DOPE/cholesterol/PEG2k**5c** = 15/15/30/2 (mol/mol)), which was consistent with the results of 4A3-SC8 DLNPs (Figure S1). We also directly compared delivery potency of five degradable dendrimer DLNPs containing Luc mRNA formulated with 4.76% PEG-DMG, 3.23% PEG2k**5a** (always on), and 3.23% PEG2k**5c** (pH-responsive), respectively (Figure 2a and S2). Interestingly, PBD-based DLNPs could deliver Luc mRNA more effectively to cells with significantly enhanced mRNA expression comparing to standard PEGDMG formulated DLNPs. Moreover, DLNPs formulated with PEG2k**5c** did not alter the cell viability (Figure S3) and could generate 5- to 35-fold more Luc protein *in vitro* than those formulated with PEGDMG (Figure 2a). Notably, 4A3-SC8 and 5A4-SC8 DLNPs enabled production of the highest level of protein both *in vitro* and *in vivo*, including 3-fold more functional Luc protein than 5A2-SC8 *in vivo* (Figure 2a, 2b, and S4). 4A3-SC8 and 5A4-SC8 could be more easily synthesized and purified than 5A2-SC8, suggesting that 4A3-SC8 and 5A4-SC8 may be useful as leading ionizable lipids for broad applications in the future.

3.2. Characterization, mechanism, and in vitro mRNA delivery

To examine the mechanism of high mRNA delivery potency using DLNPs with PBD-lipids, the physical properties of corresponding DLNPs were measured. 4A3-SC8&PEG2k**5c**, for example, could form nanoparticles uniformly, presenting an average particle diameter around 138 nm (number mean, 100 ± 5 nm), slight negative zeta potential (−1.0 mV), and a narrow polydispersity index (0.102) (Figure 2c-e). The average size of PBD-based DLNPs was 10 to 30 nm larger than DLNPs formulated with PEGDMG (Figure 2c), suggesting that the rigid planar BODIPY tail of PBD-lipids might loosen DLNP constructions and enlarge the size, but all these DLNPs exhibited similar surface charge (Figure 2c). In addition, DLNPs formulated with pH-responsive PEG2k**5c** could more effectively mediate mRNA expression in cells than “always-on” PEG2k**5a** formulated DLNPs (Figure 2a), implying that pH-activatable PBD-lipids might enhance mRNA release as the pH decreases during endosomal maturation.

To further confirm this phenomenon, we examined the capabilities of DLNPs formulated with five degradable dendrimers and different PEG-lipids for mCherry mRNA delivery. Higher mRNA delivery efficacy of PBD-based DLNPs was also observed and consistent with the results of confocal imaging (Figure 3a, 3b, and S5). To better understand the effects of PBD-lipids on mRNA delivery, hemolysis assays were conducted to compare the abilities

of DLNPs with different PEG-lipids to disrupt cell membranes in a pH-dependent manner [42]. 4A3-SC8 DLNPs were incubated with mouse blood red cells at different pH values to assess DLNP-membrane interactions during trafficking to endosomal/lysosomal compartments (Figure 3c). DLNPs formulated with PEG-DMG, PEG2k**5a**, and PEG2k**5c** exhibited low hemolytic activity at physiological pH (7.4), but achieved high hemolysis levels of 59%, 80%, and 72% at pH 5.5, respectively, demonstrating that PBD-based DLNPs possess higher membrane-disruptive properties and may assist in endosomal escape. Therefore, the larger size and faster endosomal escape of PBD-based DLNPs may both contribute to high mRNA delivery efficacy *in vitro*. Because of the uniform structural profile, smaller size compared to 5A4-SC8 DLNPs (Figure 2c), and high delivery potency, we selected 4A3-SC8 as the ionizable lipid to further investigate the effects of PBD-lipids on mRNA delivery *in vivo*.

3.3. NIR PBD DLNPs for in vivo theranostic mRNA delivery and tumor imaging

To further investigate the effects of PBD-lipids on mRNA delivery efficacy, we synthesized new PBD-lipids with an indole linker, namely PEG2k**5b**, PEG2k**5d**, PEG2k**5e**, and PEG2k**5f**, by expanding our previously reported protocols (Scheme S1) [29, 30]. The four novel PBD-lipids showed NIR emission at 724 nm, 728 nm, 738 nm, and 754 nm (Figure S6), respectively, suggesting that they are more suitable for NIR imaging *in vivo* than previously reported PEG2k**5a** (660 nm) and PEG2k**5c** (670 nm). In addition, PEG2k**5d**, PEG2k**5e**, and PEG2k**5f** were pH-responsive in water and exhibited higher pKa (5.0, 5.1, and 4.8, respectively) than PEG2k**5c** (pKa = 4.5) (Figure S7), which could be productive for tumor imaging contrast and endosomal escape.

Building on the *in vitro* mRNA delivery results, we next focused on series of PBD-lipids formulated DLNPs to deliver mRNA *in vivo*. Healthy C57BL/6 mice were injected i.v. separately with each of the six PBD-lipid&4A3-SC8 formulated DLNPs at the same dose of 0.1 mg kg^{-1} Luc mRNA and whole-body bioluminescence images were collected at 6 h post injection (Figure 4a). Strong bioluminescence was observed in mice for all DLNPs except PEG2k**5f** formulated DLNP. All six DLNPs exhibited similar surface charge (≈ −1.0 mV) and size (138 nm) except DLNP with PEG2k**5f** that had a larger size up to 165 nm (Figure S8). With respect to the effect of PEG length on PBD-lipids for mRNA delivery, we found that DLNPs formulated with PBD-lipids bearing a PEG length between 1000 and 5000 g mol^{-1} could most effectively deliver mRNA *in vivo* (Figure S9), which was consistent with prior results of PEG length effect on tumor imaging [30].

To further examine the biodistribution, main organs were collected and analyzed for bioluminescence and NIR imaging. Apart from 4A3-SC8&PEG2k**5f** DLNPs, all other DLNPs were able to productively deliver Luc mRNA to the livers (Figure 4a and 4b). Among these, PEG2k**5b** formulated DLNP enabled the highest Luc expression in the liver. Typically, DLNPs formulated with PBD-lipids containing an indole linker could more effectively deliver mRNA in the liver than those PBD-lipids with a phenoxyl linker. Moreover, the mRNA expression intensity in the liver varied significantly depending on the conjugated position of indole linker in PBD-lipid, which dramatically decreased using DLNP with PEG2k**5f**. 4A3-SC8 DLNPs containing PEG2k**5d** and PEG2k**5f** exhibited

similar surface charge (Figure S8) and pKa (Figure S10), but different size of 140 nm and 165 nm, respectively. Therefore, the larger size of DLNPs containing PEG2k**5f** might loosen DLNP construction and then reduce DLNP stability in blood circulation, resulting in lower Luc protein expression *in vivo*. We next found that 4A3-SC8 DLNPs containing PEG2k**5f**&PEGDMG exhibited a smaller size of 129 nm and recovered high mRNA delivery potency *in vivo* (Figure S11). In addition, DLNPs formulated with pH-responsive PEG2k**5c** enabling high mRNA expression *in vitro* did not exhibited higher mRNA delivery efficacy than those with "always-on" PEG2k**5a** *in vivo*, which might be caused by a slight lower pKa (Figure S10). NIR fluorescence was detected broadly in most organs, despite the fact that the mRNA was primarily expressed in the liver with minimal translation in the spleen (Figure 4a). These results indicated that DLNPs accumulated in different organs but that the mRNA was mainly translated to protein in the liver. In addition, high NIR fluorescence was observed in the lungs using DLNPs with pH-activatable PBD-lipids, whereas almost no fluorescence was displayed in the lungs using DLNPs with "always-on" PBD-lipids. The fluorescence in lung and kidneys might partially come from free PBD-lipids due to the larger size and compromised stability of DLNPs formulated with PBD-lipids bearing a rigid planar BODIPY tail (Figure S12), resulting in partial dissociation of DLNPs containing PBD-lipids in blood circulation.

Next, we examined the capabilities of DLNPs to release and produce mRNA in tumors. Mice bearing subcutaneous SUM159 breast cancer xenografts were injected with PBD-based DLNPs. Notably, PEG2k**5d** formulated DLNPs could not only enable Luc mRNA expression in the tumor but also simultaneously distinguished tumor tissues from surrounding normal tissues by virtue of pH-responsive NIR PEG2k**5d** (Figure 4c and 4d), whereas the control and "always-on" DLNPs were not able to sensitively image the tumor (Figure S13a). Moreover, 50% PEG2k**5d** and 50% PEGDMG formulated DLNPs could effectively accumulate and "turn on" in tumors, exhibiting high NIR fluorescence for 24 h after i.v. administration (Figure 4e). For i.v. administration, DLNPs with 50% PEGDMG and 50% PBD were used to decrease the size and increase tumor uptake (Figure S13b). Therefore, PBD-lipid formulated DLNPs hold great promise for NIR imaging-guided mRNA delivery to treat liver diseases and cancer.

3.4. Correlation between pKa and efficacy

To understand how PBD-lipid structure can be rationally altered to affect mRNA delivery efficacy, the surface pKa of DLNPs was measured. The surface pKa of PEG2k**5a**, PEG2k**5c**, PEG2k**5b**, PEG2k**5d**, PEG2k**5e**, and PEG2k**5f** formulated 4A3-SC8 DLNPs were 5.47, 5.17, 5.58, 5.42, 5.39, and 5.40, which were lower than the pKa of PEGDMG formulated DLNP (pKa = 6.22) (Figure S10). The slightly higher pKa of DLNPs formulated with PBD-lipids containing an indole linker compared to those PBD-lipids with a phenoxyl linker may partially explain its improved efficacy (Figure 4a and 4b). In addition, DLNPs formulated with "always-on" PBD-lipids exhibited higher pKa than those with pH-responsive PBD-lipids, which may result in higher mRNA delivery potency *in vivo*. To further examine the correlation between the intensity of mRNA expression and the pKa of DLNPs, C57BL/6 mice were injected i.v. with 0.1 mg kg^{-1} Luc mRNA in 4A3-SC8 DLNPs containing different mole ratio of PEGDMG and PEG2k**5c** (Figure 5a). Although PEG2k**5a** and

PEG2k**5b** formulated DLNPs exhibited higher mRNA expression (Figure 4a), PEG2k**5a** and PEG2k**5b** are always-on dyes. Given the pH-activatable PBDs may benefit tumor imaging by virtue of their sensitive response to pH variation, we used PEG2k**5c** as a representative PBD-lipid for pKa correlation investigation. DLNPs formulated with 100% PEGDMG exhibited the highest surface pKa of 6.22 and enabled the strongest Luc mRNA expression in the liver (Figure 5b and 5c). In contrast, DLNP formulated with 100% PEG2k**5c** exhibited the lowest surface pKa of 5.17 and showed the weakest Luc expression in the liver. Moreover, DLNP formulated with 80% PEGDMG and 20% PEG2k**5c** exhibited a lower surface pKa of 5.90, but remained almost the same Luc mRNA expression intensity as DLNP with 100% PEGDMG, demonstrating that DLNP formulated with mixed PEGDMG&PEG2k**5c** could work as a theranostic vector for NIR imaging and efficient mRNA delivery without compromised protein expression. The surface pKa of DLNP formulated with 50% PEGDMG and 50% PEG2k**5c** was 5.48, which displayed above moderate Luc mRNA expression in the liver. The four 4A3-SC8 DLNPs with PEGDMG and PEG2k**5c** exhibited similar surface charge (≈ −1.0 mV) and size (110 nm) except DLNP with only PEG2k**5c** that had a larger size up to 138 nm (Figure S14). Therefore, these results indicated that the intensity of mRNA expression in the liver was not significantly correlated with the size and surface charge, but was correlated with the pKa of DLNPs, which was also observed using DLNPs with PEGDMG and other PBD-lipids including PEG2k**5a**, PEG2k**5b**, and PEG2k**5d** (Figure S15 and S16). This is consistent with prior data on liver delivery of siRNA [43]. In addition, 5A2-SC8&PEGDMG formulated DLNPs with a surface pKa of 6.64 exhibited lower Luc expression in the liver than 4A3-SC8 DLNPs containing 100% PEGDMG (Figure S4 and S17). Thus, the PBD-lipid/PEGDMG formulated 4A3-SC8 DLNPs represent a promising theranostic platform for effective mRNA delivery to treat liver diseases, and the efficacy could be controlled by adjusting the pKa of DLNPs, indicating that DLNPs with a pKa close to 6.3 could generally produce more protein in livers (Figure S17).

4. Conclusion

In summary, we have developed a theranostic dendrimer-based LNP system containing PBD-lipids for successful mRNA delivery and NIR tumor imaging. A series of PBD-lipids was synthesized and their effects on mRNA delivery efficacy were systematically investigated *in vitro* and *in vivo*. 4A3-SC8 and 5A4-SC8 were discovered to enable more efficient mRNA delivery than previous benchmarks to cells *in vitro* and mouse livers *in vivo* after systemic administration. We further observed that DLNPs formulated with a pH-responsive PBD-lipid were more efficacious than those with PEGDMG *in vitro*, producing 5- to 35-fold more functional protein. Moreover, the relationship between PBD-lipid structure and mRNA delivery efficacy was explored, and found that DLNPs formulated with a PBD-lipid containing “always-on” BODIPY core, indole linker, and PEG length between 1000 and 5000 g/mol enabled higher mRNA delivery potency. Importantly, the correlation between the intensity of mRNA expression *in vivo* and the pKa of DLNPs was demonstrated, indicating that DLNPs with a pKa close to 6.3 could generally produce more protein in livers. Notably, 4A3-SC8&PEG2k**5d** formulated DLNP successfully mediated mRNA expression in tumors and simultaneously illuminated tumors through pH-responsive

NIR imaging. Future study will focus on the introduction of tumor suppressor proteins to treat cancer via this theranostic DLNP platform. Overall, this study not only highlights 4A3-SC8 DLNPs as a delivery vector to induce efficient functional protein expression, but also demonstrates the importance of designing and synthesizing new PEG-lipids to better understand and improve nucleic acid delivery *in vitro* and *in vivo*.

Supplementary Material

Refer to Web version on PubMed Central for supplementary material.

Acknowledgments

D.J.S. acknowledges financial support from the Department of Defense (CA150245P3), National Institutes of Health (NIH) National Cancer Institute (NCI) Cancer Center Support Grant (CCSG), NIH National Institute of Biomedical Imaging and Bioengineering (NIBIB) (R01 EB025192-01A1), American Cancer Society (ACS) (RSG-17-012-01), Cystic Fibrosis Foundation (CFF) (SIEGWA18XX0), Cancer Prevention and Research Institute of Texas (CPRIT) (R1212, RP190251), and Welch Foundation (I-1855). T.W. acknowledges financial support from the Cancer Prevention and Research Institute of Texas (CPRIT) Training Grant (RP160157). H.X. gratefully acknowledges financial support from NSFC (21907054) and Nankai University (ZB19100136). We thank Professor Angelique Whitehurst (UT Southwestern) for providing the SUM159 cell line.

References and notes

[1]. Kauffman KJ, Webber MJ, Anderson DG, Materials for non-viral intracellular delivery of messenger RNA therapeutics, J. Controlled Release 240 (2016) 227–234.

[2]. Sahin U, Kariko K, Tureci O, mRNA-based therapeutics: Developing a new class of drugs, Nat. Rev. Drug Discovery 13(10) (2014) 759–780. [PubMed: 25233993]

[3]. Hajj KA, Whitehead KA, Tools for translation: Non-viral materials for therapeutic mRNA delivery, Nat. Rev. Mater 2(10) (2017) 17056.

[4]. Kormann MS, Hasenpusch G, Aneja MK, Nica G, Flemmer AW, Herber-Jonat S, Huppmann M, Mays LE, Illenyi M, Schams A, Griese M, Bittmann I, Handgretinger R, Hartl D, Rosenecker J, Rudolph C, Expression of therapeutic proteins after delivery of chemically modified mRNA in mice, Nat. Biotechnol 29(2) (2011) 154–157. [PubMed: 21217696]

[5]. Oberli MA, Reichmuth AM, Dorkin JR, Mitchell MJ, Fenton OS, Jaklenec A, Anderson DG, Langer R, Blankschtein D, Lipid nanoparticle assisted mRNA delivery for potent cancer immunotherapy, Nano Lett. 17(3) (2017) 1326–1335. [PubMed: 28273716]

[6]. Haabeth OAW, Blake TR, McKinlay CJ, Waymouth RM, Wender PA, Levy R, mRNA vaccination with charge-altering releasable transporters elicits human T cell responses and cures established tumors in mice, Proc. Natl. Acad. Sci. U.S.A 115(39) (2018) E9153–E9161. [PubMed: 30201728]

[7]. Islam MA, Xu YJ, Tao W, Ubellacker JM, Lim M, Aum D, Lee GY, Zhou K, Zope H, Yu M, Cao WJ, Oswald JT, Dinarvand M, Mahmoudi M, Langer R, Kantoff PW, Farokhzad OC, Zetter BR, Shi JJ, Restoration of tumour-growth suppression in vivo via systemic nanoparticle-mediated delivery of PTEN mRNA, Nat. Biomed. Eng 2(11) (2018) 850–864. [PubMed: 31015614]

[8]. Miller JB, Zhang S, Kos P, Xiong H, Zhou K, Perelman SS, Zhu H, Siegwart DJ, Non-viral CRISPR/Cas gene editing in vitro and in vivo enabled by synthetic nanoparticle co-delivery of Cas9 mRNA and sgRNA, Angew. Chem. Int. Ed 56(4) (2017) 1059–1063.

[9]. Jiang C, Mei M, Li B, Zhu XR, Zu WH, Tian YJ, Wang QN, Guo Y, Dong YZ, Tan X, A non-viral CRISPR/Cas9 delivery system for therapeutically targeting HBV DNA and PCSK9 in vivo, Cell Res. 27(3) (2017) 440–443. [PubMed: 28117345]

[10]. Liu J, Chang J, Jiang Y, Meng X, Sun T, Mao L, Xu Q, Wang M, Fast and efficient CRISPR/Cas9 genome editing in vivo enabled by bioreducible lipid and messenger RNA nanoparticles, Adv. Mater 31(33) (2019) 1902575.

[11]. Hacein-Bey-Abina S, von Kalle C, Schmidt M, Le Deist F, Wulffraat N, McIntyre E, Radford I, Villeval JL, Fraser CC, Cavazzana-Calvo M, Fischer A, A serious adverse event after successful gene therapy for X-linked severe combined immunodeficiency, New Engl. J. Med 348(3) (2003) 255–256. [PubMed: 12529469]

[12]. Perez-Ortin JE, Alepuz P, Chavez S, Choder M, Eukaryotic mRNA decay: Methodologies, pathways, and links to other stages of gene expression, J. Mol. Biol 425(20) (2013) 3750–3775. [PubMed: 23467123]

[13]. Fenton OS, Kauffman KJ, McClellan RL, Appel EA, Dorkin JR, Tibbitt MW, Heartlein MW, DeRosa F, Langer R, Anderson DG, Bioinspired alkenyl amino alcohol ionizable lipid materials for highly potent in vivo mRNA delivery, Adv. Mater 28(15) (2016) 2939–2943. [PubMed: 26889757]

[14]. Fenton OS, Kauffman KJ, Kaczmarek JC, McClellan RL, Jhunjhunwala S, Tibbitt MW, Zeng MD, Appel EA, Dorkin JR, Mir FF, Yang JH, Oberli MA, Heartlein MW, DeRosa F, Langer R, Anderson DG, Synthesis and biological evaluation of ionizable lipid materials for the in vivo delivery of messenger RNA to B lymphocytes, Adv. Mater 29(33) (2017) 1606944.

[15]. Fenton OS, Kauffman KJ, McClellan RL, Kaczmarek JC, Zeng MD, Andresen JL, Rhym LH, Heartlein MW, DeRosa F, Anderson DG, Customizable lipid nanoparticle materials for the delivery of siRNAs and mRNAs, Angew. Chem. Int. Ed 130(41) (2018) 13770–13774.

[16]. Kauffman KJ, Dorkin JR, Yang JH, Heartlein MW, DeRosa F, Mir FF, Fenton OS, Anderson DG, Optimization of lipid nanoparticle formulations for mRNA delivery in vivo with fractional factorial and definitive screening designs, Nano Lett. 15(11) (2015) 7300–7306. [PubMed: 26469188]

[17]. Li B, Luo X, Deng B, Wang J, McComb DW, Shi Y, Gaensler KM, Tan X, Dunn AL, Kerlin BA, Dong Y, An orthogonal array optimization of lipid-like nanoparticles for mRNA delivery in vivo, Nano Lett. 15(12) (2015) 8099–8107. [PubMed: 26529392]

[18]. Uchida H, Itaka K, Nomoto T, Ishii T, Suma T, Ikegami M, Miyata K, Oba M, Nishiyama N, Kataoka K, Modulated protonation of side chain aminoethylene repeats in N-substituted polyaspartamides promotes mRNA transfection, J. Am. Chem. Soc 136(35) (2014) 12396–12405. [PubMed: 25133991]

[19]. Kaczmarek JC, Patel AK, Kauffman KJ, Fenton OS, Webber MJ, Heartlein MW, DeRosa F, Anderson DG, Polymer-lipid nanoparticles for systemic delivery of mRNA to the lungs, Angew. Chem. Int. Ed 55(44) (2016) 13808–13812.

[20]. Yan Y, Xiong H, Zhang X, Cheng Q, Siegwart DJ, Systemic mRNA delivery to the lungs by functional polyester-based carriers, Biomacromolecules 18(12) (2017) 4307–4315. [PubMed: 29141136]

[21]. Sabnis S, Kumarasinghe ES, Salerno T, Mihai C, Ketova T, Senn JJ, Lynn A, Bulychev A, McFadyen I, Chan J, A novel amino lipid series for mRNA delivery: Improved endosomal escape and sustained pharmacology and safety in non-human primates, Mol. Ther 26(6) (2018) 1509–1519. [PubMed: 29653760]

[22]. Benner NL, McClellan RL, Turlington CR, Haabeth OAW, Waymouth RM, Wender PA, Oligo(serine ester) charge-altering releasable transporters: Organocatalytic ring-opening polymerization and their use for in vitro and in vivo mRNA delivery, J. Am. Chem. Soc 141(21) (2019) 8416–8421. [PubMed: 31083999]

[23]. Cheng Q, Wei T, Jia Y, Farbiak L, Zhou K, Zhang S, Wei Y, Zhu H, Siegwart DJ, Dendrimer-based lipid nanoparticles deliver therapeutic FAH mRNA to normalize liver function and extend survival in a mouse model of hepatorenal tyrosinemia type I, Adv. Mater 30(52) (2018) e1805308. [PubMed: 30368954]

[24]. Akinc A, Maier MA, Manoharan M, Fitzgerald K, Jayaraman M, Barros S, Ansell S, Du X, Hope MJ, Madden TD, Mui BL, Semple SC, Tam YK, Ciufolini M, Witzigmann D, Kulkarni JA, van der Meel R, Cullis PR, The Onpattro story and the clinical translation of nanomedicines containing nucleic acid-based drugs, Nat. Nanotechnol 14(12) (2019) 1084–1087. [PubMed: 31802031]

[25]. Ramishetti S, Hazan-Halevy I, Palakuri R, Chatterjee S, Naidu Gonna S, Dammes N, Freilich I, Kolik Shmuel L, Danino D, Peer D, A combinatorial library of lipid nanoparticles for RNA delivery to leukocytes, Adv. Mater 32(12) (2020) e1906128. [PubMed: 31999380]

[26]. Zhou K, Nguyen LH, Miller JB, Yan Y, Kos P, Xiong H, Li L, Hao J, Minnig JT, Zhu H, Siegwart DJ, Modular degradable dendrimers enable small RNAs to extend survival in an aggressive liver cancer model, Proc. Natl. Acad. Sci. U.S.A 113(3) (2016) 520–525. [PubMed: 26729861]

[27]. Cheng Q, Wei T, Farbiak L, Johnson LT, Dilliard SA, Siegwart DJ, Selective ORgan Targeting (SORT) nanoparticles for tissue specific mRNA delivery and CRISPR/Cas gene editing, Nat. Nanotechnol 15(4) (2020) 313–320. [PubMed: 32251383]

[28]. Mui BL, Tam YK, Jayaraman M, Ansell SM, Du XY, Tam YYC, Lin PJC, Chen S, Narayanannair JK, Rajeev KG, Manoharan M, Akinc A, Maier MA, Cullis P, Madden TD, Hope MJ, Influence of polyethylene glycol lipid desorption rates on pharmacokinetics and pharmacodynamics of siRNA lipid nanoparticles, Mol. Ther. - Nucl. Acids 2 (2013) e139.

[29]. Xiong H, Kos P, Yan Y, Zhou K, Miller JB, Elkassih S, Siegwart DJ, Activatable water-soluble probes enhance tumor imaging by responding to dysregulated pH and exhibiting high tumor-to-liver fluorescence emission contrast, Bioconjugate Chem. 27(7) (2016) 1737–1744.

[30]. Xiong H, Zuo H, Yan Y, Occhialini G, Zhou K, Wan Y, Siegwart DJ, High-contrast fluorescence detection of metastatic breast cancer including bone and liver micrometastases via size-controlled pH-activatable water-soluble probes, Adv. Mater 29(29) (2017) 1700131.

[31]. Akinc A, Goldberg M, Qin J, Dorkin JR, Gamba-Vitalo C, Maier M, Jayaprakash KN, Jayaraman M, Rajeev KG, Manoharan M, Koteliansky V, Roehl I, Leshchiner ES, Langer R, Anderson DG, Development of lipidoid-siRNA formulations for systemic delivery to the liver, Mol. Ther 17(5) (2009) 872–879. [PubMed: 19259063]

[32]. Alabi CA, Love KT, Sahay G, Yin H, Luly KM, Langer R, Anderson DG, Multiparametric approach for the evaluation of lipid nanoparticles for siRNA delivery, Proc. Natl. Acad. Sci. U.S.A 110(32) (2013) 12881–12886. [PubMed: 23882076]

[33]. Cullis PR, Hope MJ, Lipid nanoparticle systems for enabling gene therapies, Mol. Ther 25(7) (2017) 1467–1475. [PubMed: 28412170]

[34]. Paunovska K, Sanchez AJD, Sago CD, Gan ZB, Lokugamage MP, Islam FZ, Kalathoor S, Krupczak BR, Dahlman JE, Nanoparticles containing oxidized cholesterol deliver mRNA to the liver microenvironment at clinically relevant doses, Adv. Mater 31(14) (2019) 1807748.

[35]. Patel S, Ashwanikumar N, Robinson E, Xia Y, Mihai C, Griffith JP 3rd, Hou S, Esposito AA, Ketova T, Welsher K, Joyal JL, Almarsson O, Sahay G, Naturally-occurring cholesterol analogues in lipid nanoparticles induce polymorphic shape and enhance intracellular delivery of mRNA, Nat. Commun 11(1) (2020) 983. [PubMed: 32080183]

[36]. Kulkarni JA, Witzigmann D, Leung J, Tam YYC, Cullis PR, On the role of helper lipids in lipid nanoparticle formulations of siRNA, Nanoscale 11(45) (2019) 21733–21739. [PubMed: 31713568]

[37]. Zhou K, Johnson LT, Xiong H, Barrios S, Minnig JT, Yan Y, Abram B, Yu X, Siegwart DJ, Hydrophobic domain structure of linear-dendritic poly(ethylene glycol) lipids affects RNA delivery of lipid nanoparticles, Mol. Pharmaceut 17(5) (2020) 1575–1585.

[38]. Kedmi R, Veiga N, Ramishetti S, Goldsmith M, Rosenblum D, Dammes N, Hazan-Halevy I, Nahary L, Leviatan-Ben-Arye S, Harlev M, Behlke M, Benhar I, Lieberman J, Peer D, A modular platform for targeted RNAi therapeutics, Nat. Nanotechnol 13(3) (2018) 214–219. [PubMed: 29379205]

[39]. Weinstein S, Toker IA, Emmanuel R, Ramishetti S, Hazan-Halevy I, Rosenblum D, Goldsmith M, Abraham A, Benjamini O, Bairey O, Raanani P, Nagler A, Lieberman J, Peer D, Harnessing RNAi-based nanomedicines for therapeutic gene silencing in B-cell malignancies, Proc. Natl. Acad. Sci. U.S.A 113(1) (2016) E16–22. [PubMed: 26699502]

[40]. Zhang S, Nguyen LH, Zhou K, Tu HC, Sehgal A, Nassour I, Li L, Gopal P, Goodman J, Singal AG, Yopp A, Zhang Y, Siegwart DJ, Zhu H, Knockdown of anillin actin binding protein blocks cytokinesis in hepatocytes and reduces liver tumor development in mice without affecting regeneration, Gastroenterology 154(5) (2018) 1421–1434. [PubMed: 29274368]

[41]. Zhang S, Zhou K, Luo X, Li L, Tu HC, Sehgal A, Nguyen LH, Zhang Y, Gopal P, Tarlow BD, Siegwart DJ, Zhu H, The polyploid state plays a tumor suppressive role in the liver Dev. Cell 44(4) (2018) 447–459.

[42]. Cheng C, Convertine AJ, Stayton PS, Bryers JD, Multifunctional triblock copolymers for intracellular messenger RNA delivery, Biomaterials 33(28) (2012) 6868–6876. [PubMed: 22784603]

[43]. Jayaraman M, Ansell SM, Mui BL, Tam YK, Chen JX, Du XY, Butler D, Eltepu L, Matsuda S, Narayanannair JK, Rajeev KG, Hafez IM, Akinc A, Maier MA, Tracy MA, Cullis PR, Madden TD, Manoharan M, Hope MJ, Maximizing the potency of siRNA lipid nanoparticles for hepatic gene silencing in vivo, Angew. Chem. Int. Ed 51(34) (2012) 8529–8533.

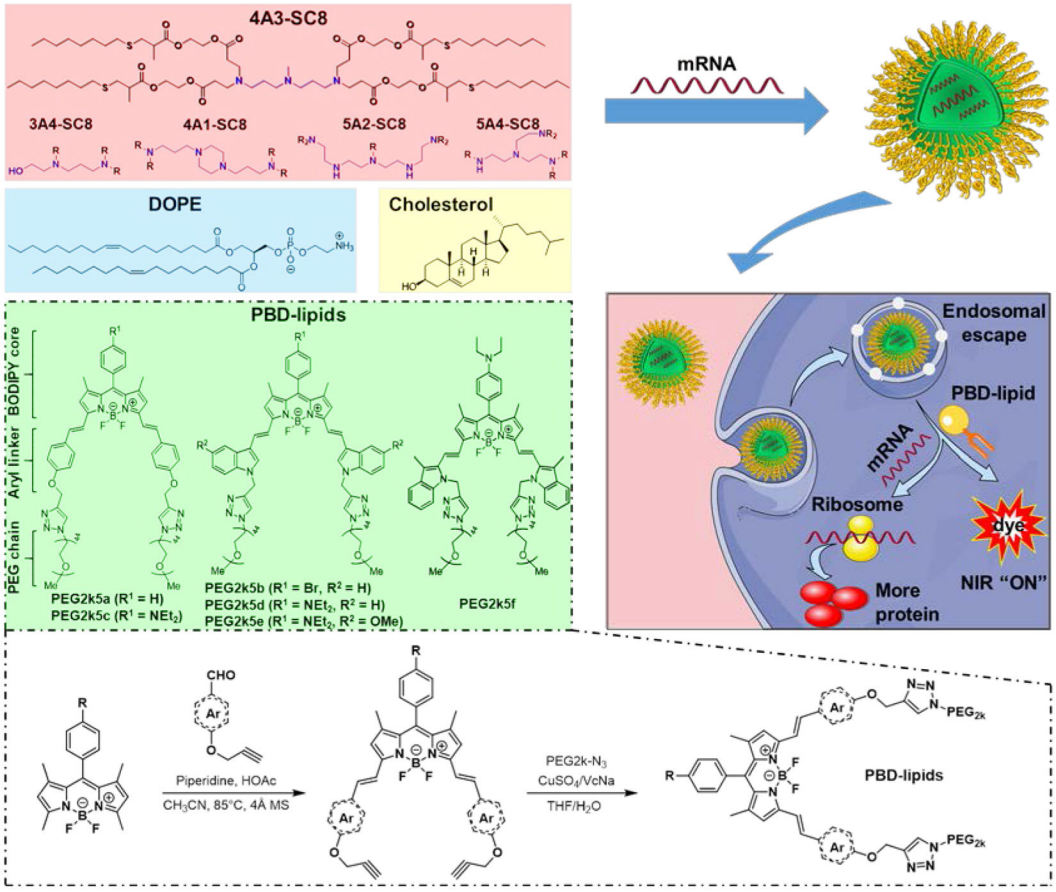

Figure 1.

Schematic illustration of formulated dendrimer/DOPE/cholesterol/PBD-lipid/mRNA nanoparticles for theranostic mRNA delivery. A series of PBD-lipids was created and formulated into dendrimer lipid nanoparticles (DLNPs) that enabled intracellular mRNA delivery, expression of target proteins and activation of pH-responsive PBD in cancer cells. All PBD-lipids except PEG2k**5a** and PEG2k**5b** are ionizable lipids.

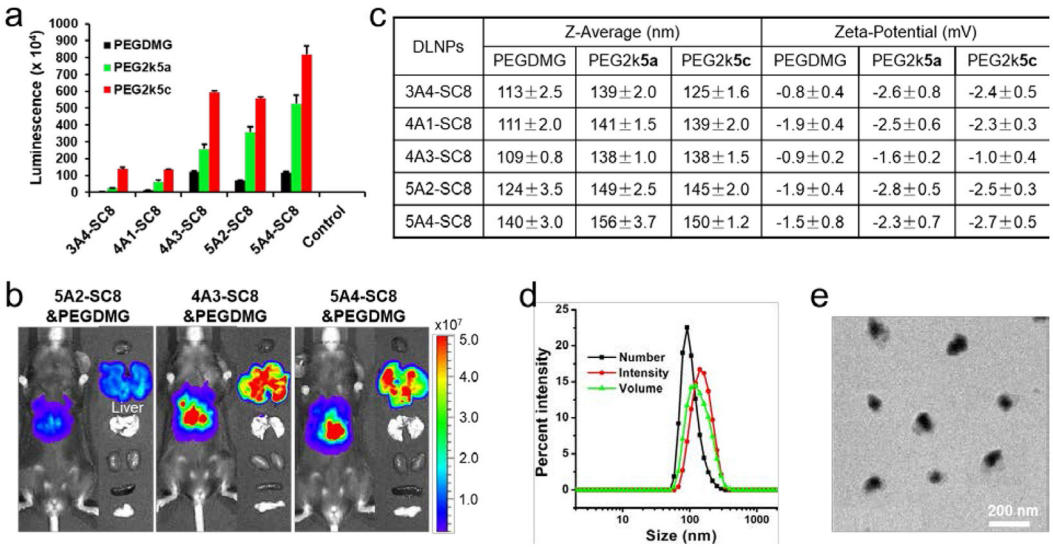

c

DLNPs	Z-Average (nm)			Zeta-Potential (mV)		
	PEGDMG	PEG2k**5a**	PEG2k**5c**	PEGDMG	PEG2k**5a**	PEG2k**5c**
3A4-SC8	113±2.5	139±2.0	125±1.6	-0.8±0.4	-2.6±0.8	-2.4±0.5
4A1-SC8	111±2.0	141±1.5	139±2.0	-1.9±0.4	-2.5±0.6	-2.3±0.3
4A3-SC8	109±0.8	138±1.0	138±1.5	-0.9±0.2	-1.6±0.2	-1.0±0.4
5A2-SC8	124±3.5	149±2.5	145±2.0	-1.9±0.4	-2.8±0.5	-2.5±0.3
5A4-SC8	140±3.0	156±3.7	150±1.2	-1.5±0.8	-2.3±0.7	-2.7±0.5

Figure 2.

PBD-based DLNPs exhibited high delivery potency of luciferase mRNA in cells. **a**) Luminescence intensity of IGROV1 cells treated with different DLNP formulations containing luciferase mRNA 24 h after transfection (25 ng mRNA per well; mean ± s.d., n = 3). Control: untreated cells. **b**) C57BL/6 mice were injected intravenously with different DLNPs formulated with PEGDMG at a dose of 0.1 mg kg^{-1} Luc mRNA and imaged 6 h after injection. **c**) Z-Average size and zeta potential of DLNPs formulated with 4.76 % PEGDMG, 3.23% PEG2k**5a**, and 3.23% PEG2k**5c**, respectively. **d**) DLS size of 4A3-SC8&PEG2k**5c** DLNP. **e**) TEM image of 4A3-SC8&PEG2k**5c** DLNP.

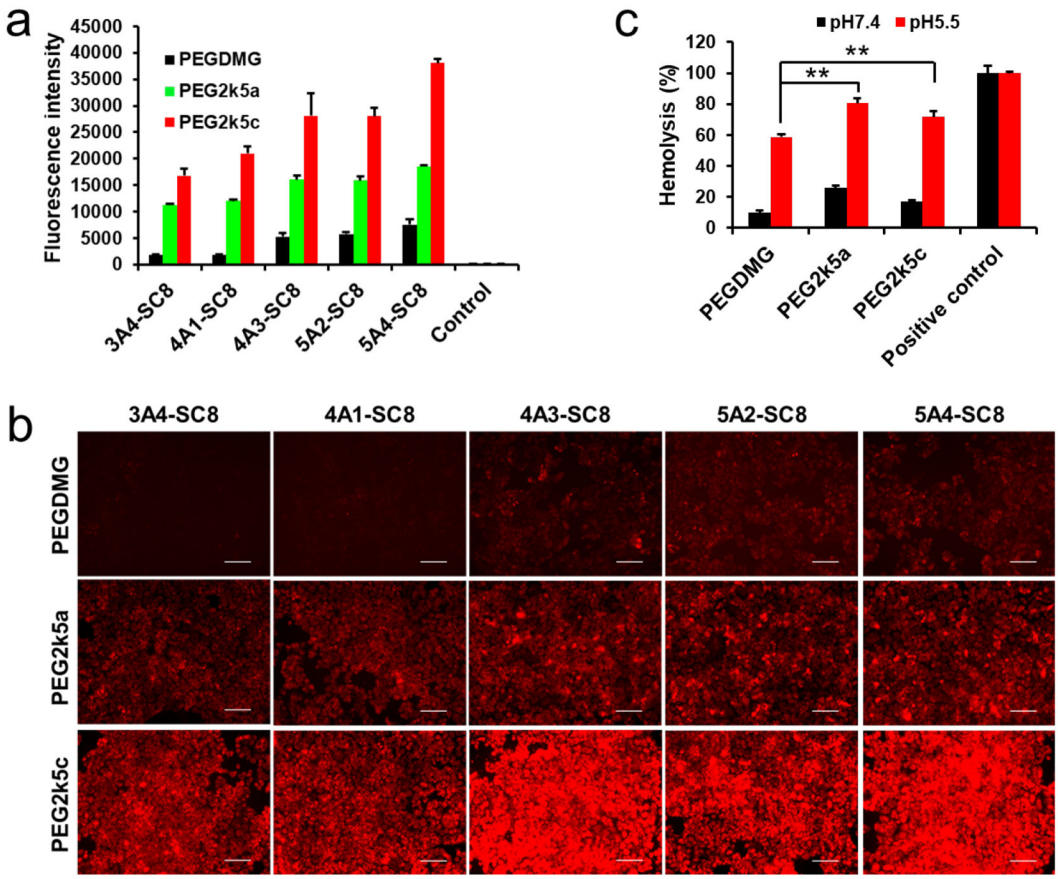

Figure 3.

PBD-based DLNPs enhanced mCherry mRNA expression in cytoplasm. **a**) Fluorescence intensity of IGROV1 cells treated with different DLNP formulations containing mCherry mRNA 24 h after transfection (80 ng mRNA per well; mean ± s.d., n = 3). Control: untreated cells. **b**) Fluorescence images of IGROV1 cells 24 h after treatment with mCherry mRNA DLNPs at a dose of 80 ng mRNA/well. Scale bar: 100 μm. **c**) Hemolysis of 4A3-SC8 DLNPs with varying PEG-lipids at different pH. Positive control: 1% triton X-100. Statistical significance was determined using a two-tailed Student's *t* test (**, P ≤ 0.01).

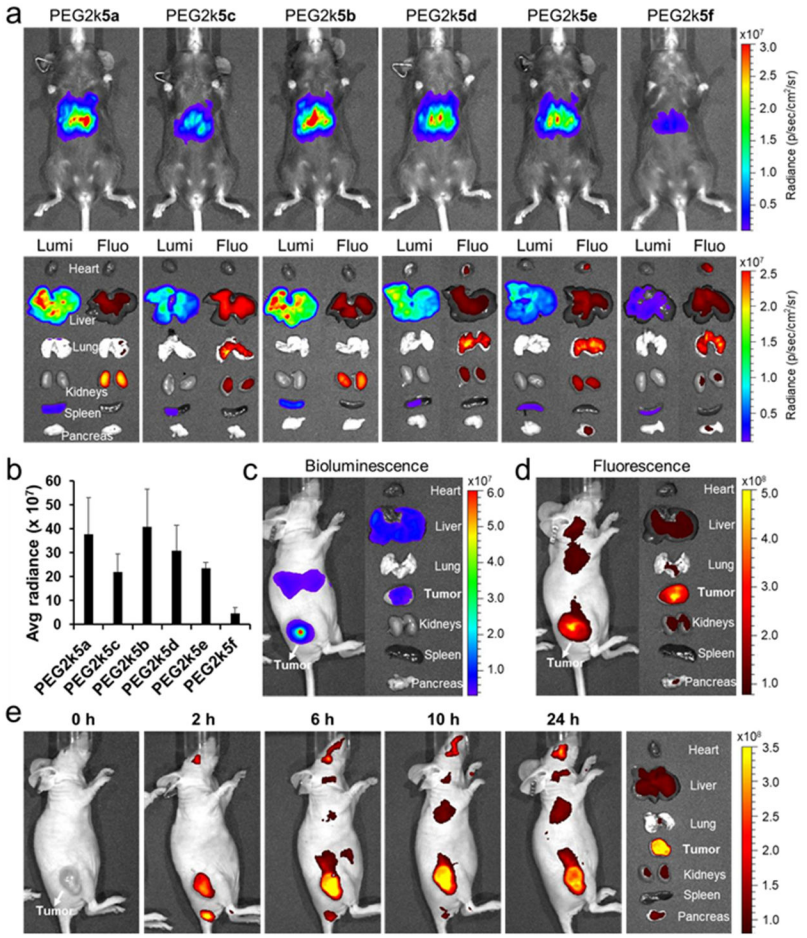

Figure 4.

In vivo evaluation of PBD-lipid effects on mRNA delivery. **a**) C57BL/6 mice were injected i.v. separately with the series of six 4A3-SC8 DLNPs formulated with different PBD-lipids at the same dose of 0.1 mg kg^{-1} Luc mRNA and imaged by IVIS after 6 h (n = 2). Then organs were collected for bioluminescence and fluorescence imaging. **b**) Quantification of *ex vivo* Luc mRNA expression intensity in livers. **c**) Subcutaneous SUM159 breast tumor-bearing mice were injected intratumorally with 4A3-SC8&PEG2k**5d** DLNP at a dose of 0.05 mg kg^{-1} Luc mRNA and imaged by bioluminescence and fluorescence (**d**) at 6 h post injection. Representative *ex vivo* bioluminescence (**c**) and fluorescence (**d**) images of harvested tumor and organs from SUM159 breast tumor-bearing mice sacrificed at 6 h post injection. (**e**) Time-dependent *in vivo* fluorescence images of mice bearing subcutaneous SUM159 breast cancer xenograft tumors after i.v. injection of 0.2 mg kg^{-1} Luc mRNA loaded 4A3-SC8 DLNPs containing 50% PEGDMG & 50% PEG2k**5d**. Representative fluorescence images of harvested tumors and organs from SUM159 tumor-bearing mice sacrificed at 24 h post injection.

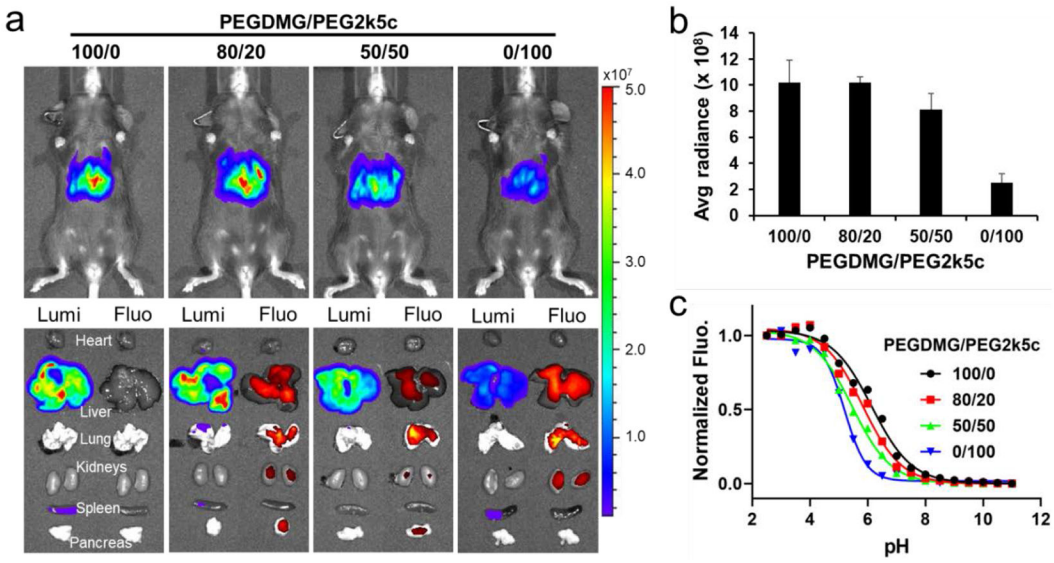

Figure 5.

The intensity of mRNA expression *in vivo* correlated with the pKa of DLNPs. **a**) C57BL/6 mice were injected i.v. with 0.1 mg kg^{-1} Luc mRNA in 4A3-SC8 DLNPs containing different mole ratio of PEGDMG and PEG2k**5c** (n = 2). Bioluminescence was quantified 6 h after injection. **b**) Quantification of Luc mRNA expression intensity in livers. **c**) The pKa of PEGDMG/PEG2k**5c** formulated 4A3-SC8 DLNPs.